Biochemical Pharmacology 98 (2015) 69–77

Contents lists available at ScienceDirect

Biochemical Pharmacology

journal homepage: www.elsevier.com/locate/biochempharm

Quantitative evaluation of cellular uptake, DNA incorporation and adduct formation in cisplatin sensitive and resistant cell lines: Comparison of different Pt-containing drugs

M. Corte-Rodríguez[a], M. Espina[b], L.M. Sierra[b], E. Blanco[a,*], T. Ames[c], M. Montes-Bayón[a,*], A. Sanz-Medel[a]

[a] Department of Physical and Analytical Chemistry, Faculty of Chemistry, University of Oviedo, C/ Julian Clavería 8, 33006 Oviedo, Spain
[b] Department of Functional Biology (Genetics Area) and Oncology University Institute (IUOPA), University of Oviedo, Spain
[c] Phosplatin Therapeutics, New York, NY, United States

ARTICLE INFO

Article history:
Received 12 June 2015
Accepted 31 August 2015
Available online 6 September 2015

Keywords:
Cisplatin
Oxaliplatin
Pyrodach-2
Cell lines
ICP-MS
DNA
Adduct formation

ABSTRACT

The use of Pt-containing compounds as chemotherapeutic agents facilitates drug monitoring by using highly sensitive elemental techniques like inductively coupled plasma mass spectrometry (ICP-MS). However, methodological problems arise when trying to compare different experiments due to the high variability of biological parameters. In this work we have attempted to identify and correct such variations in order to compare the biological behavior of cisplatin, oxaliplatin and pyrodach-2 (a novel platinum-containing agent). A detailed study to address differential cellular uptake has been conducted in three different cell lines: lung adenocarcinoma (A549); cisplatin-sensitive ovarian carcinoma (A2780); and cisplatin-resistant ovarian carcinoma (A2780cis). The normalization of Pt results to cell mass, after freeze-drying, has been used to minimize the errors associated with cell counting. Similarly, Pt accumulation in DNA has been evaluated by referencing the Pt results to the DNA concentration, as measured by ^{31}P monitoring using flow-injection and ICP-MS detection. These strategies have permitted to address significantly lower Pt levels in the resistant cells when treated with cisplatin or oxaliplatin as well as an independent behaviour from the cell type (sensitive or resistant) for pyrodach-2. Similarly, different levels of incorporation in DNA have been found for the three drugs depending on the cell model revealing a different behavior regarding cell cisplatin resistance. Further speciation experiments (by using complementary HPLC–ICP-MS and HPLC–ESI-Q-TOF MS) have shown that the main target in DNA is still the N7 of the guanine but with different kinetics of the ligand exchange mechanism for each of the compounds under evaluation.

1. Introduction

The search for new chemotherapeutic drugs that overcome the limitations associated with the use of traditional treatments, such as cisplatin acquired drug resistance, is an area of continuous investigation [1,2]. In this regard, the use of alternatives such as carboplatin and oxaliplatin has been explored in numerous cancerous processes, and these therapies are nowadays in wide use [3,4]. The mechanism of action of these drugs is believed to rely first on the drug uptake by the cells followed by its transport within the cytosol to the cell nucleus where its interaction with the DNA generates the so-called Pt–DNA adducts [5]. These adducts are formed by sequential substitution of the ligands initially present within the drug structure followed by final drug–DNA binding producing several monodentate adducts, as well as many intra- and inter-strand cross links [6,7]. The intra-strand DNA complexes, where Pt bridges adjacent guanine bases, is by far the most dominant DNA adduct with both cisplatin and oxaliplatin, comprising approx. 65% of the total number of adducts [8]. The resulting adduct formation is believed to result in an inhibition of the replication and transcription leading to subsequent cell death [9]. Thus, the efficacy of a given treatment is thought to be highly dependent on the degree of formation of such adducts which is also cell-type dependent [10].

However, there are several limiting factors affecting the formation of Pt–DNA adducts [11]. The first one is related to the drug uptake from the growth media (in the case of in vitro test systems) into cells. It has been observed by some authors that the

* Corresponding author. Tel.: +34 985103478; fax: +34 985103125.
E-mail address: montesmaria@uniovi.es (M. Montes-Bayón).

http://dx.doi.org/10.1016/j.bcp.2015.08.112
0006-2952/

cellular incorporation of cisplatin (the most studied Pt–drug) is limited to approximately 1% of the total drug concentration used for exposure [12]. Interestingly, reduced drug accumulation is frequently observed in cisplatin-resistant cell lines, such as A2780cis, although the mechanism responsible for this effect remains difficult to assess [13]. It could result either from a reduced drug uptake from the culture media (due to alterations in some specific membrane transporters) [14] or enhanced drug efflux, or both. A second limiting factor is that once incorporated into the cells, the drug can be inactivated by binding to different biomolecules present within the cell cytosols (e.g., glutathione, proteins, etc.) [15]. The final outcome is that very little Pt from the initial concentration used for exposure finally reaches the target molecule, the DNA. In any in vivo system, this effect is further determined by the drug's stability in plasma. Lastly, once formed, the Pt–DNA adducts can be also repaired by specific enzymes that recognize the DNA damage [16]. The degree of tolerance to persisting (unrepaired) DNA lesions determines the fate of a given cell, which may be survival or apoptosis.

In an attempt to design new platinum compounds to overcome the above described cisplatin limitations, some authors have designed many metallodrugs, including those containing other metallic ions such as ruthenium [17] or different types of ligands in the case of Pt-based therapies [18,19]. An example of this latter case is the development of a family of anionic platinum complexes that seem to act at the cell level but avoiding penetration into the cell nucleus named phosphaplatins. Phosphaplatins [20,21] are a family of compounds containing a diaminocyclohexane core structure (similar to that of oxaliplatin) but with a pyrophosphate group as ligand instead of oxalate. These compounds have exhibited superior efficacy with reduced toxicity in several cellular models, and one member of the family, pyrodach-2, is currently in clinical development [21]. These pyrophosphate complexes seem to have different cellular and molecular antitumor mechanisms compared to conventional platinum therapeutics. In order to understand these mechanisms more completely, work regarding drug uptake, incorporation into DNA or formation of DNA–Pt adducts, in comparison to more conventional Pt–drugs in different types of cell cultures would be desirable.

The present study attempts to establish adequate analytical methodologies that permit comparison of the outcome of different chemotherapeutic treatments by monitoring parameters such as cellular uptake, DNA platination and DNA adduct formation. Methodological strategies that permit the analysis of micro-samples in combination with ICP-MS as a Pt selective detector [22] are optimized here in order to conduct the quantitative evaluation of the cellular uptake and DNA incorporation of cisplatin, oxaliplatin and a model phosphaplatin compound (pyrodach-2) (Fig. 1). The study was simultaneously conducted in three different cell lines which are model for cancer types in which Pt-therapy is almost the standard treatment: cisplatin-sensitive ovarian cancer (A2780), cisplatin-resistant ovarian cancer (A2780cis), and lung adenocarcinoma (A549). The normalization of the Pt concentration results to biological parameters such as the number of cells or the DNA concentration within the cell nucleus was evaluated. Secondly, speciation experiments have been also done in order to address the structure of the possible DNA–Pt interactions of the three drugs by applying capillary HPLC and simultaneous ICP-MS and ESI-Q-TOF MS for detection [23,24].

2. Materials and methods

2.1. Reagents

All chemicals were of analytical reagent grade or better. Ultrapure water (>18 MΩ) obtained from a Milli-Q system (Millipore, Bedford, MA, USA) was used throughout. Working standard solutions were prepared daily by solubilization of the solid compounds in ultrapure water and 10 mM $NaHCO_3$ for pyrodach-2. Calf thymus DNA (lyophilized powder) and Nuclease S1 from *Aspergillus oryzae* were purchased from Sigma–Aldrich (St. Louis, MO, USA). Cisplatin (*cis*-diamminedichloroplatinum(II)), oxaliplatin (1,2-diaminocyclohexane oxalate platinum(II)) and pyrodach-2 (1,2-diaminocyclohexane pyrophosphate platinum (II)) were kindly provided by Phosplatin Therapeutics as highly-pure active pharmaceutical powder from a single manufacturing source (Heraeus GmbH, Hanau, Germany). For cell culture, Dulbecco's modified Eagle's medium (DMEM), PBS and trypsin were from LabClinics (Barcelona, Spain), RPMI 1640 medium and fetal bovine serum were from Invitrogen (Fisher Scientific, Madrid, Spain) and plasmocin was from InvivoGen (San Diego, USA). Nitric acid (65%, Suprapur quality) and hydrogen peroxide (30%) were

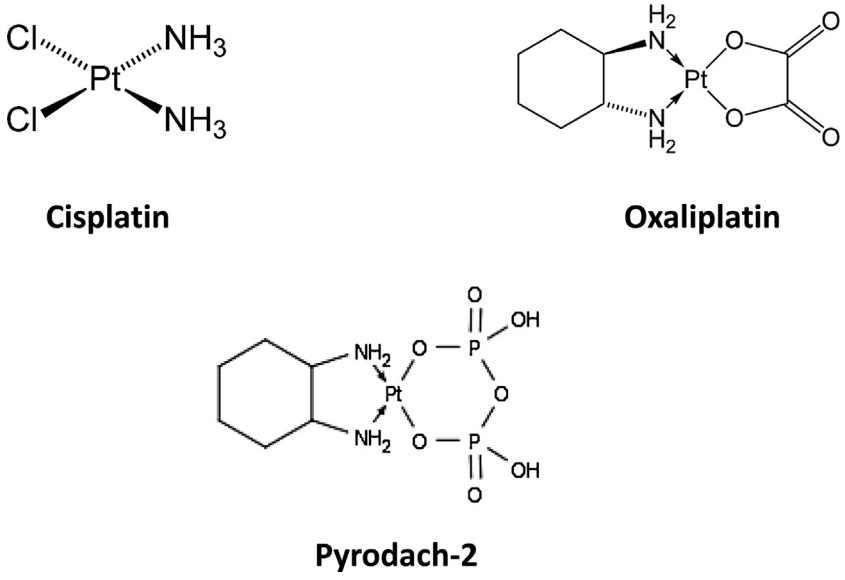

Fig. 1. Chemical structure of the different compounds used for the incubation experiments.

purchased by Merck Millipore (Darmstadt, Germany). Ammonium acetate (Sigma–Aldrich), ammonium hydroxide solution (28% w/v) (Merck Millipore) for the preparation of HPLC mobile phases and sodium bicarbonate (for solubilisation of pyrodach-2, pH 7.2 in the final stock solution) (Merck Millipore) were used. The oligo 5′-TCCGGTCC-3′ used for incubation with the different Pt containing drugs was obtained from Invitrogen. Incubations were conducted for 24 h in an excess of oligo (5:1) and the resulting product was digested using Nuclease S1 as described elsewhere [7].

2.2. Instrumentation

Flow injection experiments were conducted in the ICP-MS Thermo X-Series^{II} (Thermo Fisher Scientific, Bremen, Germany) fitted with a concentric pneumatic nebulizer and a conical spray chamber. Flow injection analysis mode was always used to minimize sample consumption. For this aim, the instrument peristaltic pump was applied with a constant flow of 1 mL/min and using 2% HNO_3 as carrier. Sample injection was conducted using a dual mode injection valve from Rheodyne, model 9125 (Cotati, California, USA), fitted with a 50 μL PEEK injection loop (Upchurch Scientific, Oak Harbor, Washington, USA). Spectrophotometric measurements of DNA were taken in a Nanodrop 2000c UV–vis (Thermo).

For the speciation studies, the capillary column ZORBAX Eclipse SB-C18 (150 × 0.3 mm id, 5 μm) (Agilent Technologies, Japan) was used, coupled either to the ICP-MS Element 2 (Thermo Fisher Scientific) or to the quadrupole-time-of-flight spectrometer (ESI-Q-TOF MS) QStar XL (Applied Biosystem, Langen, Germany) operated in the positive ionization mode and fitted with a MicroSpray® ion source and using N_2 as the nebulization gas. The ICP-MS was fitted with a DS-5 total consumption nebulizer (CETAC Technologies, Omaha, Nebraska, USA) and a self-developed spray chamber.

2.3. Cell culture conditions

A549 adenocarcinoma human alveolar basal epithelial cell line and A2780 human ovarian carcinoma cell line were kind gifts from Dr. J.M. Pérez Freije (Department of Biochemistry and Molecular Biology, University of Oviedo); the in vitro derived cisplatin-resistant A2780cis cell line was purchased from the European collection of cell cultures through Sigma–Aldrich. The cells were cultured at 37 °C in a 5% CO_2 incubator using DMEM medium for the A549 cell line and RPMI 1640 medium for the A2789 and A2780cis cell lines, both media were supplemented with 10% foetal bovine serum and 5 mg L^{-1} of plasmocin. The cell cultures were exposed to cisplatin, oxaliplatin and pyrodach-2 at 5, 10 and 20 μM respectively for 3 h at 37 °C, afterwards they were washed with PBS (5 times) and collected by trypsinization. In order to obtain a homogeneous contact between the drugs and the cells, solutions containing the desired drug concentration were made up to volume in the growth media. The initially used cell culture media was then replaced by the media containing the drug of interest. Non-drug treated cells (control cells) were also processed alongside the drug treated cells. Cells (approximately 9×10^6 cells) were divided into two aliquots (1/3 for Pt determination in whole cells and 2/3 for DNA extraction).

For evaluation of Pt uptake in whole cells, the cell pellet was first lyophilized (by freeze-drying) and then weighed in a high precision (±0.01 mg) balance (New ClassicMS105DU, Mettler Toledo, Spain). Afterwards, 500 μL of 65% HNO_3 (Suprapur, Merck) were added to the freeze dried pellet and the mixture was heated at 70 °C for 1 h in a water bath. After this time, 500 μL of 30% H_2O_2 were added to the mixture and left at 70 °C for 3 h more. The transparent solution was then transferred to a small vial for further dilution in order to conduct Pt determination by ICP-MS.

2.4. Extraction and purification of genomic DNA

Genomic DNA was extracted and purified from all the cultured cells (from about 6×10^6 cells per extraction) using the silica-based column DNA purification kit PureLink™ Genomic DNA Mini Kit (Invitrogen, Carlsbad, USA). The kit was used according to the manufacturer's instructions with the inclusion of RNAse A treatment to generate RNA-free genomic DNA. The extracted DNA was eluted using 100 μL of the elution buffer (10 mM Tris–HCl, pH 9.0, 0.1 mM EDTA).

DNA purity was confirmed by comparing the ratio of UV measurements at 260 and 280 nm with the ratio of pure DNA standards, which should be between 1.7 and 1.9. The concentration of isolated DNA was determined by measuring UV absorbance at 260 nm assuming that one absorbance unit equals 50 μg mL^{-1} for double stranded DNA. Additionally, DNA concentration was also assessed by ^{31}P monitoring using ICP-MS after sample digestion using a similar protocol than that previously described for whole cell analysis but, in this case, using 100 μL of HNO_3 (65%) and 60 μL

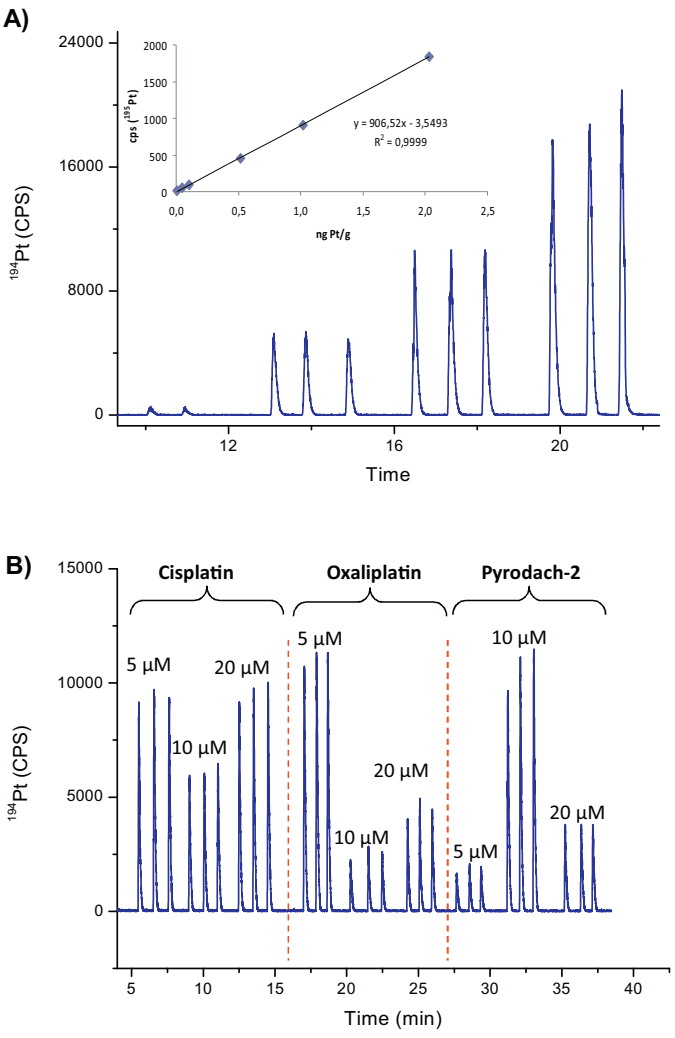

Fig. 2. Flow injection-ICP-MS of Pt (A) flow injection profile and calibration curve (inset) obtained for Pt standards (0–2 ng/g Pt) and (B) injection of the cell cultures (line A549) after incubation with the different Pt-compounds and acid digestion of the cells using the conditions detailed in the manuscript.

of H_2O_2 (30%). Sample was further diluted 1:10 for analysis. A ^{31}P calibration curve was constructed by applying the same digestion procedure to commercially available calf thymus DNA (Sigma).

3. Results

3.1. Platinum determination in whole cells

For the characterization of the analytical method based on FIA-ICP-MS, a calibration curve with standards ranging from 0.01 to 2 ng g^{-1} Pt was constructed, as can be observed in Fig. 2(A). The method detection limit turned out to be 0.005 ng g^{-1} Pt which seems to be adequate for the purpose of quantification of Pt in cells, and the %RSD for three independent injections of the same solution was about 2–3%. In addition, to prove that the cell acid digestion was adequate and that no matrix effects were remaining, control cells were digested according to the previously described procedure and spiked afterwards with different Pt concentrations. The plot of added Pt vs. found Pt showed a slope of 1.06 ($r^2 = 0.98$, data not shown), confirming that the matrix effects under these conditions, if any, were negligible. Once the most important methodological features were established, the first experiments to address Pt drug uptake by cancer cells were performed using the cell line A549 (lung cancer). For the aim of this study, fresh cells (approximately 9×10^6) were divided into two aliquots corresponding approximately to 3×10^6 cells (for total cellular uptake studies) and 6×10^6 cells (for analysis of Pt in DNA). The same experiment was repeated for the three Pt–drugs (cisplatin, oxaliplatin and pyrodach-2) at 5, 10 and 20 μM. Fig. 2(B) shows the results obtained (raw data) by flow injection with ICP-MS detection after acid digestion of the fresh samples. In order to improve the accuracy of the measurement, the Pt counts where then normalized to the cell mass that was obtained by weighing the freeze-dried cell pellet. The cell mass obtained for the different experiments ranged from 1.5 to 2.3 mg dry weight (a difference as high as 65%) which could, indeed, be the source of the variability in results reported in Fig. 2(B). Fig. 3(A–C) shows the observed Pt concentration results but normalized to the dry cell mass in the different cell lines and for the different studied compounds. In Fig. 3(A) the incorporation results obtained for the line A549 is given for the three compounds and follows the sequence cisplatin > oxaliplatin > pyrodach-2 at each concentration with a difference of 10-fold in incorporation levels from cisplatin to pyrodach-2. In all cases, the Pt incorporation increases linearly with exposure doses for each of the three drugs.

In Fig. 3(B) the incorporation results for A2780 and A2780cis are provided after exposure to cisplatin and oxaliplatin respectively. In this case, the cisplatin resistant cell line (A2780cis) exhibits lower levels of Pt incorporation (up to 10-fold) than the sensitive line in the case of cisplatin exposure and about 5-fold in the case of oxaliplatin exposure. Finally, Fig. 3(C) shows the obtained results for pyrodach-2 in these two cell models (presented in a different scale for clarity). In this case, the incorporation levels are below 1 μg/g cell (significantly lower than for the other two Pt–drugs) and independent of the cell line (sensitive or resistant to cisplatin) or exposure concentration used.

3.2. Platinum determination in DNA of exposed cells

Since the target molecule for most Pt drugs is primarily the nuclear DNA, specific determination of Pt in DNA was conducted by extracting DNA from the exposed cells. As in the case of the whole cell analysis, Pt concentration was normalized to the DNA concentration, which was initially measured spectrophotometrically at 260 nm. It is now conventional to assert that an aqueous solution of double-stranded DNA with an optical density (OD) of

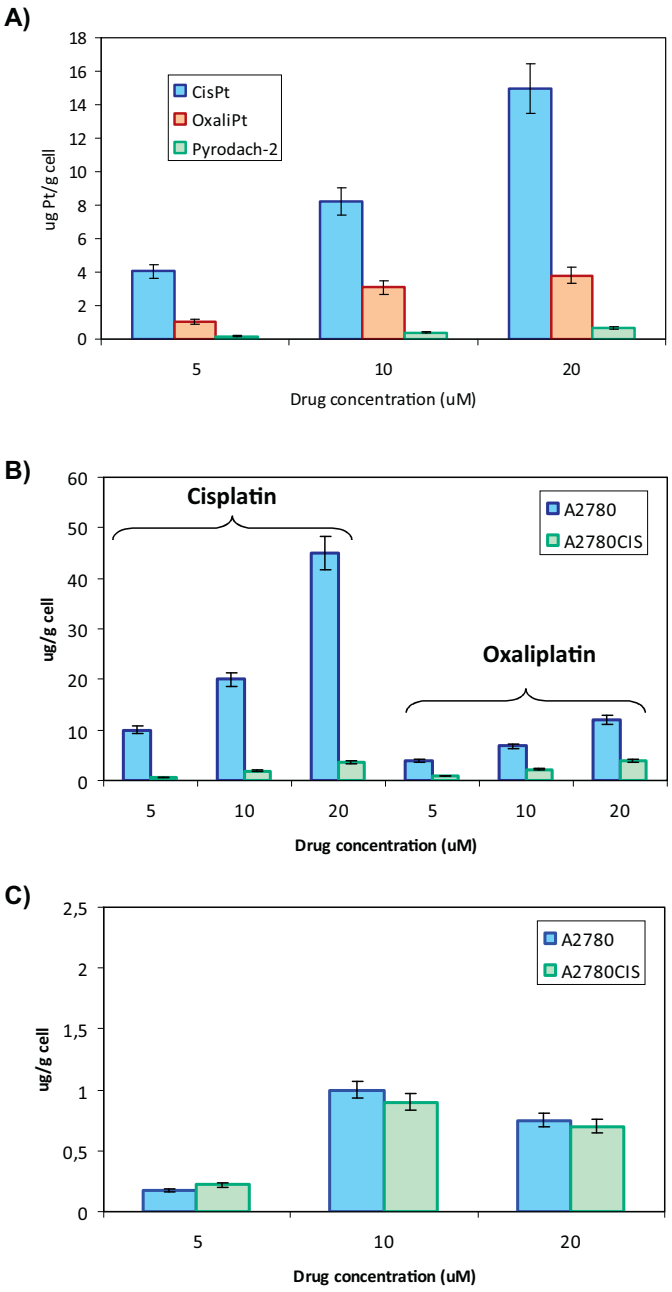

Fig. 3. Quantitative results of the Pt incorporated into the cells (A) A549 treated with different concentrations of the three Pt compounds, (B) A2780 and A2780cis treated with cisplatin and oxaliplatin, (C) A2780 and A2780cis treated with pyrodach-2. Results expressed as μg/g dry cell.

1.0 at 260 nm in a 1 cm pathlength cuvette has a [DNA] of 50 μg/mL (50 ng/μL) [25]. However, intact DNA shows a high viscosity that might compromise the absorbance measurements when the solution is not completely homogeneous. This situation might also represent a source of variation when comparing different treatments in different cell cultures, and therefore additional precautions were taken for avoiding such variations. To this aim, calf thymus DNA (lyophilized standard) was solubilised in water and acid digested using the previously detailed conditions modified from Zayed et al. [10]. Dilutions of the digestion product were analysed using the FI-ICP-MS previously described, monitoring ^{31}P, and the obtained results can be seen in Fig. 4(A). This method has the advantage that the obtained P signal can be

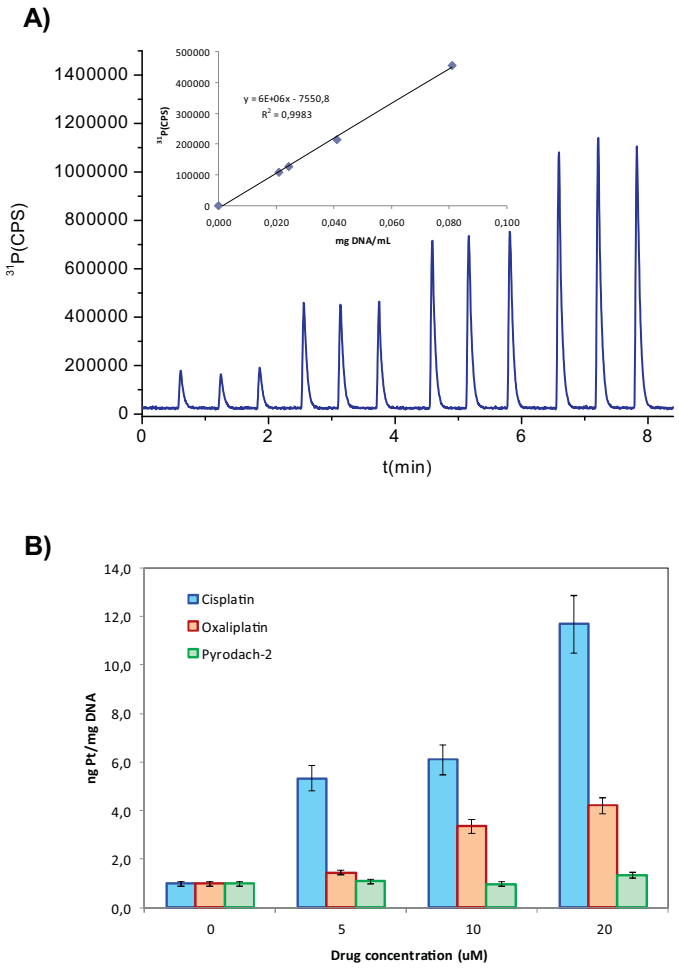

Fig. 4. (A) Flow injection profiles of DNA standards (calf thymus DNA) after acid digestion and calibration curve (inset) of ^{31}P vs. mg DNA/mL and (B) quantitative results of Pt incorporation in DNA from the different Pt-containing drugs in the A549 cell line.

directly correlated to DNA concentration in the standard and, therefore, in the samples once digested in the same way.

In order to address the suitability of the proposed methodology, a set of samples ($n = 5$) were analysed using the two strategies (spectrophotometry and ICP-MS) after DNA extraction. The plot of both sets of results (data not shown) showed a slope of 1.19 ($r^2 = 0.85$) revealing a poor correlation among experimental data. Therefore, for simplicity, further measurements of DNA samples were conducted by FI-ICP-MS, simultaneously to the Pt measurement. In this regard, Fig. 4(B) shows the obtained ng Pt/mg DNA for the cell line A549 exposed to the three drugs at different concentrations. Results in cell lines A2780 and A2780cis for the three drugs are shown in Fig. 5 (A2780 solid colors and A2780cis striped pattern colors). In the light of these results, the first observation is that Pt incorporation into DNA is much more efficient in the case of cisplatin than for the other Pt drugs in all the studied cell models and, in particular, in the sensitive ovarian line (A2780). In the latter case, Pt concentration results were about 4.5 fold if compared to oxaliplatin and 10 fold if compared to pyrodach-2. Regarding drug concentration, at 5 and 10 μM, oxaliplatin and pyrodach-2 exhibited comparable incorporation levels. However, significant differences could be observed at 20 μM. In the resistant cell line, the values are significantly lower for all the compounds and it is remarkable that the incorporation levels of cisplatin and oxaliplatin are indistinguishable from each other at all assayed doses.

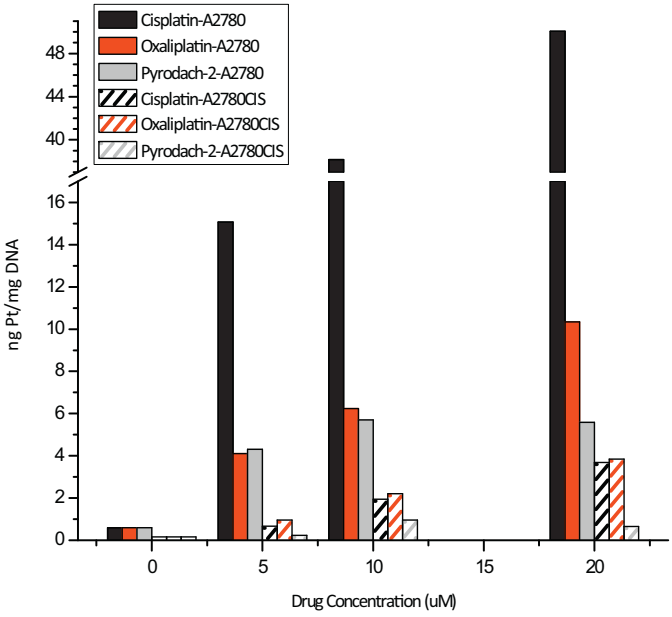

Fig. 5. Quantitative results of Pt incorporation in DNA from the different Pt-containing drugs in the A2780 and A2780cis (cisplatin sensitive and resistant respectively) cell lines using 5, 10 and 20 μM drug concentration in all cases.

The mass balance of the Pt for the three drugs was also conducted, starting from the Pt clearance from the culture media after cell exposure. For this aim, the Pt concentration in the culture media before and after exposure to cells was determined. The observation was that the Pt concentration decreases after cell exposure (independently from the type of drug, concentration and cell line), by about 10%. However, by comparing these levels with those obtained in the exposed cells it is clear that not all the Pt is incorporated into cells. In fact, only 3% (cisplatin), 1% (oxaliplatin) and 0.1% (pyrodach-2) of the concentration used for exposure has been found inside the cells (calculated for A2780 cell line at 20 μM). These values are significantly reduced in the case of the resistant cell model, where just 0.4%, 0.5% and 0.2% incorporation rate was obtained for cisplatin, oxaliplatin and pyrodach-2, respectively. The rest is probably adsorbed into the plastic bottles used for cell growing as reported by other authors [26].

In addition, the normalization of the Pt–DNA data to whole cell Pt-levels calculated for A2780 and A2780cis at 20 μM provided the results given in Table 2. As can be seen, cisplatin and oxaliplatin show a very similar behaviour in both, sensitive and resistant cell models exhibiting comparable DNA-incorporation levels of about 1% in the sensitive line and about 3% in the resistant one. On the other hand, pyrodach-2 reflects analogous results in both lines with incorporation ratios higher (5% vs. 1% or 3%) than the other two drugs.

3.3. Structure of DNA adducts with cisplatin, oxaliplatin and pyrodach-2 by MS

In order to evaluate the structure of the adducts formed between the three drugs and DNA, a model oligonucleotide which contained a GG pair (most efficient binding partner of hydrolysed cisplatin, as demonstrated in previous studies) [7,22] was chosen for incubation with the drugs. Incubations of the three drugs with an excess of oligonucleotide were conducted, followed by the enzymatic hydrolysis of the reaction product using Nuclease S1. The obtained products were separated by reverse phase chromatography (capillary) coupled on-line with ICP-MS and ESI-Q-TOFMS. The obtained chromatograms corresponding to the incubations of cisplatin,

Table 1
Instrumental operating conditions for the ICP-MS, the chromatographic system and ESI-MS measurements.

Parameter	ICP-MS (Thermo X-Series^{II})
RF Power	1400 W
Isotopes monitored	^{194}Pt, ^{195}Pt
Nebulizer	DS 5
Spray chamber	4 °C
OctP bias	–
HexP bias	−0.5 V
QP bias	−6.5 V

Parameter	LC (Agilent 1100)
Flow rate	6 μL min^{-1}
Sheath flow	–
Injection volume	2 μL
Column	Agilent Zorbax SB C_{18}
Particle size	5 μm
Dimensions	0.5 × 150 mm
Mobile phase A	2% MeOH, 0.1% formic acid
Mobile phase B	98% MeOH, 0.1% formic acid
Gradient	0–50% B (in 30 min)
	50% (30–35 min)

Parameter	ESI-Q-TOF MS (QStar XL)
Mode	Positive
Ionspray voltaje	5.5 kV
Nebulizing gas	N_2
Sample flow rate	6 μL min^{-1}
Calibration	Renin standard
Scan range	*m*/*z* 200–1300

oxaliplatin and pyrodach-2 are shown in Fig. 6(A–C, respectively) using ICP-MS detection (elemental Pt monitoring). As can be observed, cisplatin generates mainly one adduct eluting at 19 min (Fig. 6A) that according to ESI-Q-TOF MS shows a molecular mass at *m*/*z* 452.5622 (shown in Fig. 7A) corresponding to the cisplatin-GG adduct doubly charged (difference with the theoretical mass 8 ppm). The monocharged species have been also detected in the mass spectrometer (e.g., see *m*/*z* 904.13) but with much lower intensity. This could be due to the slightly acidic conditions of the mobile phase used as well as the ionization conditions in the source (see Table 1). Previous quantitative experiments revealed that the formation of this adduct (main Pt containing species) accounts for approximately 75% of the incubated cisplatin [9].

The results are slightly different in the case of using oxaliplatin or pyrodach-2 as metallodrugs. In these cases, several Pt-containing species are coming from the column showing same retention times (although different intensities). This is not surprising if the structure of the two compounds is observed (see Fig. 1), since the hydrolysed species (replacing the oxalate or the pyrophosphate ligands by other molecules) can be similar under certain conditions. However, in the ICP-MS signal can be seen that the most abundant species in the case of oxaliplatin interaction with the oligo is the one at 20.5 min (see Fig. 6B), which according to ESI-Q-TOF MS, corresponds also to the oxaliplatin-GG (also doubly charged) with a molecular mass at *m*/*z* 492.5980 (6 ppm with the theoretical mass, see Fig. 7B). In the case of pyrodach-2, this peak corresponds to only the second most abundant species. The most abundant one elutes at 24.6 min (present also in both traces of Fig. 6B and C) showing a molecular ion of *m*/*z* 783.0660 (singly charged) that contains Pt-isotope pattern (shown in Fig. 7C). According to our calculations, this could correspond to a derivative of the pyrodach-2-GG in which one of the nucleobases has been eliminated, together with the

Table 2
Platinum mass ratio (ng in DNA in respect to the ng in the whole cell) calculated for the sensitive (A2780) and resistant (A2780cis) cell models exposed to 20 μM of cisplatin, oxaliplatin and pyrodach-2, respectively.

Drug	Cell line	ng Pt in DNA/ng intracellular Pt (%)
Cisplatin	A2780	1.1 ± 0.1
	A2780cis	3.3 ± 0.4
Oxaliplatin	A2780	0.9 ± 0.1
	A2780cis	3 ± 1
Pyrodach-2	A2780	5 ± 1
	A2780cis	5 ± 1

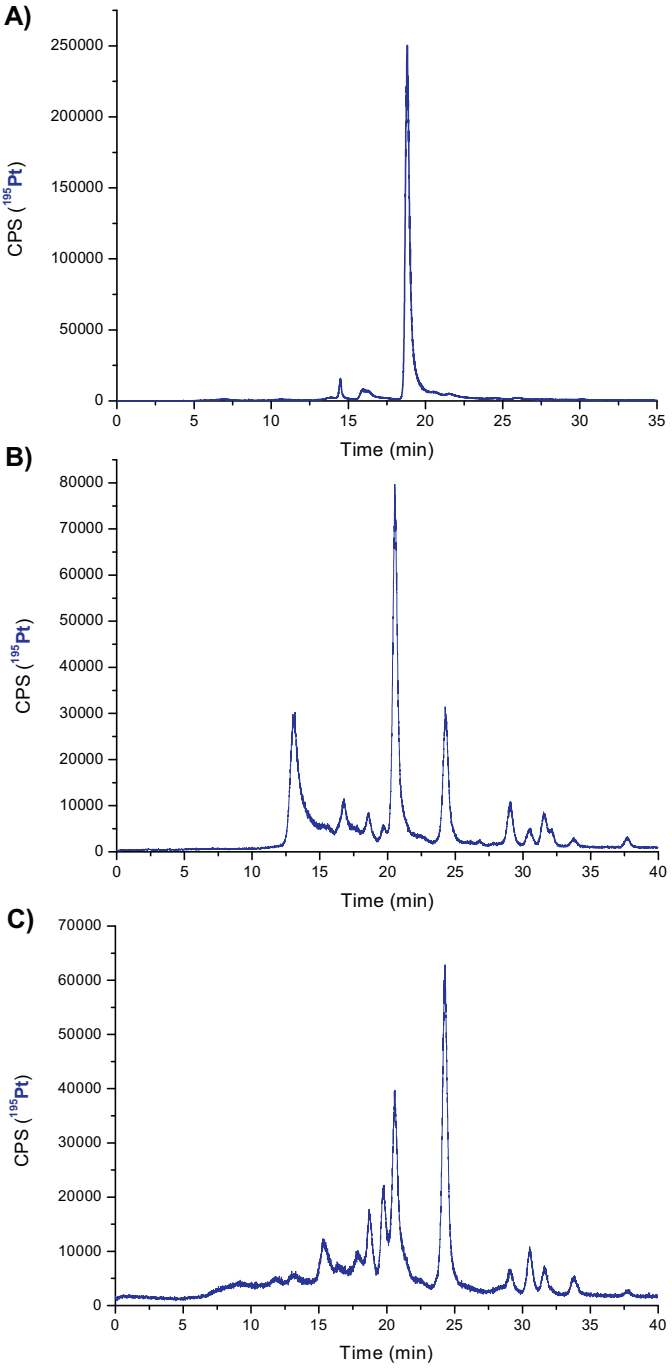

Fig. 6. Platinum traces obtained for the incubation of the oligonucleotide (3′-TCCGGTCC-5′) with cisplatin (A), oxaliplatin (B) and pyrodach-2 (C) after enzymatic digestion with nuclease S1 by coupling capillary liquid chromatography to ICP-MS.

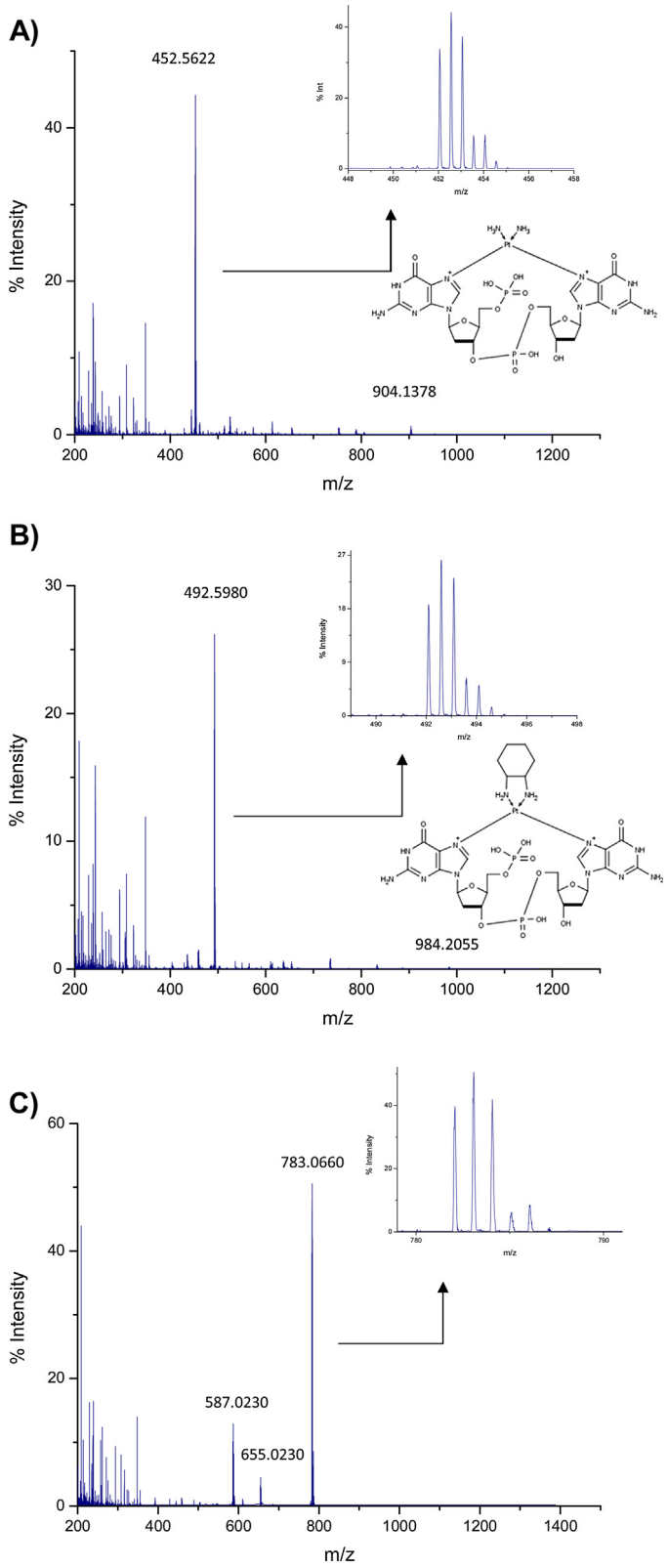

Fig. 7. Mass spectra obtained by capillary LC-ESI-q-TOF of the compounds obtained from the incubation of (3′-TCCGGTCC-5′) with cisplatin (at 19.5 min in Fig. 6) (A), oxaliplatin (21 min in Fig. 6) (B) and pyrodach-2 (24.5 min in Fig. 6) (C) after enzymatic digestion with nuclease S1. The insets show also the structure of the adducts obtained for cisplatin and oxaliplatin, respectively.

1,2-diaminocyclohexane, and a bicarbonate molecule (used as solubilisation media for the pyrodach-2) is bound to Pt (proposed

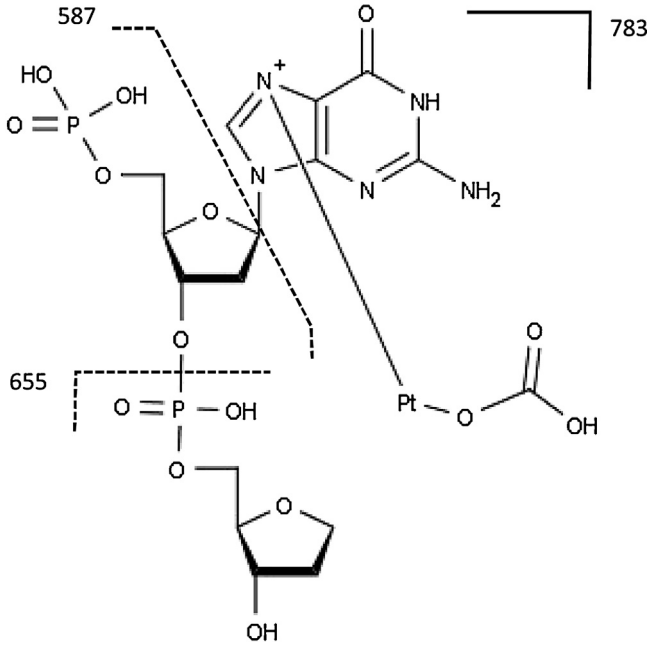

Fig. 8. Chemical structure of the obtained main adduct between pyrodach-2 and the oligonucleotide.

structure in Fig. 8). This structure could be ascribed to an initial bifunctional adduct between Pt and the two adjacent guanosines (main target in DNA also for the other two drugs) which further evolved to form a stable structure with a counterpart like bicarbonate (used for the solubilisation of this compound) [23].

These kind of reaction intermediates have been also observed in the case of cisplatin in previous studies [27] and can be strongly dependent on the ligand exchange reaction that is taking place during the adduct formation. The structure proposed is also supported by the presence of other ions at the same retention time and corresponding to the additional loss of one deoxyribose + phosphate molecules (m/z 587.0230) coming, most likely, by in-source fragmentation of the molecule. Additional experiments conducted by MS/MS (data not shown) confirmed this hypothesis.

4. Discussion

Accurate comparison among cell cultures and Pt drugs requires specific normalization to biological parameters such as number of cells or DNA concentration. Regarding the number of cells, several alternatives have been presented in the literature including the normalization of the Pt results to the protein concentration (spectrophotometrically measured) or to the cells weight after freeze drying of the cell pellet (once the remaining growth media is decanted). Using the second type of experiment, it was possible to ascribe the individual variations observed in the Pt raw signals to differences in the number of cells taken for each experiment (cell counting could be used as an approximation). Thus, further concentration results are normalized to the cells weight.

On the view of Pt incorporation in the different cell models, it can be concluded that the incorporation of Pt from pyrodach-2 into all the cell models assayed is considerably lower than for cisplatin and oxaliplatin. Interestingly, in the resistant cell line both drugs (cisplatin and oxaliplatin) exhibit very similar incorporation results. However, in the case of pyrodach-2, the incorporated Pt seems to be independent of the cell type (sensitive or resistant cell lines showed similar results) and of the exposure concentrations. These results point out that pyrodach-2 does not seem to be

affected by the same resistance mechanism that affects both cisplatin and oxaliplatin, while cell apoptosis following pyrodach-2 treatment appears to be taking place, according to previous publications [20]. These results, taken together with the apoptosis data suggest a different mechanism of action than cellular uptake and direct binding of the pyrodach-2 to DNA, as proposed by other authors [21]. Therefore, the drug shows promising capabilities in cisplatin resistant models.

In addition, the comparative results of Pt incorporation in the two cell lines of ovarian cancer (A2780 and A2780cis) treated with cisplatin and oxaliplatin points out that the cell resistance can be ascribed, to some extent, to a decrease in the intracellular drug concentration (since significantly lower intracellular Pt concentrations have been obtained in the resistant model for both compounds). Additional experiments are necessary to address if this is due to a decreased uptake or an increased export mechanism. Regarding oxaliplatin, a significant decrease in drug incorporation can be also seen in the resistant line with respect to the sensitive one probably ascribed to developed cross-resistance that other authors have reported in cisplatin resistant cell models [28].

Regarding Pt incorporation into DNA, some contamination issues were encountered during Pt determination since Pt concentrations in the control samples of about 1 ng/mg DNA were found. These values indicate some minor contamination problems either during sample preparation or sample introduction into the ICP-MS. Therefore, for addressing concentration levels below 1 ng/mg DNA, special precautions should be taken into account. Here, as in the analysis of whole cells, in the resistant cell line, the values are significantly lower for all the compounds and is remarkable that the incorporation levels of cisplatin and oxaliplatin are indistinguishable from each other at all assayed doses confirming the possible cross-resistance. Incorporation of Pt from pyrodach-2 in DNA shows a different trend, as in the case of cellular incorporation, independent of the exposure concentration. However, reliable conclusions regarding DNA affinity of the three compounds can only be taken if a Pt-mass balance is conducted in the cells. For this purpose, the obtained data of Pt in DNA needs to be normalized to the uptake levels of Pt in whole cells.

When normalizing the Pt-DNA data to whole cell Pt-levels at 20 μM for the three compounds (see Table 2), the results show that, in this cell model, resistance to cisplatin is related to a decrease in intracellular drug concentration rather than to the inactivation of the drug due to the presence of binding partners within the cell cytosol (since the resistant cell line shows even higher percentage of DNA incorporation than the sensitive one). Since ICP-MS provides compound independent response, the speciation experiments conducted (Fig. 6) point out that the formation of cisplatin adducts with DNA is highly specific (basically a single Pt-containing peak is detected) and quantitatively formed. In addition, the ESI-Q-TOFMS confirms that such structure corresponds to the binding at the N7 of the guanine to form the bidentate adduct with the sequence GG as main reaction product. These experiments reveal, on the other hand, not such a specific binding in the case of oxaliplatin (see Figs. 6B) where presence of other less intense Pt-containing adducts seems evident and the intensity of the formed GG adduct is considerably lower than in the case of cisplatin (even when similar Pt starting concentrations have been used for incubation).

On the other hand, although pyrodach-2 seems to be poorly incorporated into cells, the little incorporated fraction seems to be efficiently associated to DNA (with percentages of 5% in both cell models). However, in this cell model DNA incorporation of pyrodach-2 seems to be independent of the cell type (as already seen in the cellular incorporation results of Fig. 3C). In any case, in the absence of data to specifically isolate the nuclear components, it is important to address that this findings do not necessarily mean that pyrodach-2 has an increased DNA affinity. It could mean that it is more efficiently absorbed into the nucleus to facilitate interaction with nuclear DNA. When speciation analysis is conducted using ICP-MS (Fig. 6C) is possible to address the formation of a number of different Pt-containing adducts (comparable to the case of oxaliplatin), some of them unidentified. The adduct formed between the drug and the pair GG (at 20.5 min) is not the most abundant one, in this case. A possible explanation is that the ligand exchange mechanism (necessary for having the drug in the active form to interact with DNA) exhibits slower reaction kinetics that in the case of having oxalate ligands as in the case of oxaliplatin. Thus, other reaction intermediates can be detected by ESI-Q-TOF like this one at m/z 783.0660 (see Fig. 7C).

When the cellular and Pt-DNA incorporation results are compared in light of the efficacy data of pyrodach-2 and cisplatin, both in A2780cis cells (cisplatin IC-50: 20.5 μM vs. pyrodach-2 IC-50: 2.5 μM) and in A549 cells (cisplatin IC-50: 2.8 μM vs. pyrodach-2 IC-50: 0.9 μM) some conclusions can be extracted. First, that although some Pt-DNA interactions can be detected in cells, the more realistic possibility is that pyrodach-2 anti-cancer activity results from mechanisms independent of cellular accumulation or DNA interaction associated with the traditional platinum agents. Thus, an apoptotic mechanism related to the binding of this drug to specific targets in the cellular membrane, as a differential aspect to the other two drugs could be proposed. This consideration may be further underlined by ongoing anti-proliferation studies conducted separately by Phosplatin Therapeutics.

Acknowledgments

The authors want to thank Phosplatin Therapeutics (in particular M. Price, T. Ames and W. Luke) for their collaboration during the development of the investigations and for fruitful discussions. The funding through the projects CTQ2013-49032-C2-1-R (MINECO) and FC-15-GRUPIN14-010 (FICYT) as well as the grant of M. Corte (FICYT BP13114) are gratefully acknowledged.

References

[1] R. Agarwal, S.B. Kaye, Ovarian cancer: strategies for overcoming resistance to chemotherapy, Nat. Rev. Cancer 3 (2003) 502–516.
[2] N.R. Patel, B.S. Pattni, A.H. Abouzeid, V.P. Torchilin, Nanopreparations to overcome multidrug resistance in cancer, Adv. Drug Deliv. Rev. 65 (2013) 1748–1762.
[3] M.A. Graham, G.F. Lockwood, D. Greenslade, S. Brienza, M. Bayssas, E. Gamelin, Clinical pharmacokinetics of qxaliplatin: a critical review, Clin. Cancer Rev. 6 (2000) 1205–1218.
[4] A. Ardizzoni, L. Boni, M. Tiseo, F.V. Fossella, J.H. Schiller, M. Paesmans, D. Radosavljevic, A. Paccagnella, P. Zatloukal, P. Mazzanti, D. Bisset, R. Rosell, Cisplatin-versus carboplatin-based chemotherapy in first-line treatment of advance non-small-cell lung cancer, J. Natl. Cancer Inst. 99 (2007) 847–857.
[5] S.E. Sherman, D. Gibson, A.H. Wang, S.J. Lippard, X-ray structure of the major adduct of the anticancer drug cisplatin with DNA: *cis*-[Pt(NH_3)$_2$(d(pGpG))], Science 230 (1985) 412–417.
[6] S.G. Chaney, S.L. Campbell, E. Bassett, Y. Wu, Recognition and processing of cisplatin- and oxaliplatin–DNA adducts, Crit. Rev. Oncol. 53 (2005) 3–11.
[7] D. Garcia-Sar, M. Montes-Bayón, E. Blanco-González, A. Sanz-Medel, Speciation studies of *cis*-platin adducts with DNA nucleotides via elemental specific detection (P and Pt) using liquid chromatography-inductively coupled plasma-mass spectrometry and structural characterization by electrospray mass spectrometry, J. Anal. At. Spectrom. 21 (2006) 861–868.
[8] A. Eastman, The formation, isolation and characterization of DNA adducts produced by anticancer platinum complexes, Pharmacol. Ther. 34 (1987) 155–166.
[9] D. García Sar, L. Aguado, M. Montes-Bayón, M.A. Comendador, E. Blanco González, A. Sanz-Medel, L.M. Sierra, Relationships between cisplatin-induced adducts and DNA strand-breaks, mutation and recombination in vivo in somatic cells of *Drosophila melanogaster*, under different conditions of nucleotide excision repair, Mutat. Res. 741 (2012) 81–88.
[10] A. Zayed, T. Shoeib, S.E. Taylor, G.D.D. Jones, A.L. Thomas, J.P. Wood, H.J. Reid, B. L. Sharp, Determination of Pt–DNA adducts and the sub-cellular distribution of Pt in human cancer cell lines and the leukocytes of cancer patients, following

mono or combination treatments, by ICP-MS, Int. J. Mass Spectrom. 307 (2011) 70–78.
[11] M. Kartalou, J.M. Essigmann, Mechanisms of resistance to cisplatin, Mutat. Res. 478 (2001) 23–43.
[12] C.R. Centerwall, K.A. Tacka, D.J. Kerwood, J. Goodisman, B.B. Toms, R.L. Dubowy, J.C. Dabrowiak, Modification and uptake of a cisplatin carbonato complex by Jurkat cells, Mol. Pharmacol. 70 (2006) 348–355.
[13] V. Schneider, M.L. Krieger, G. Bendas, U. Jaehde, G.V. Kalayda, Contribution of intracellular ATP to cisplatin resistance of tumor cells, J. Biol. Inorg. Chem. 18 (2013) 165–174.
[14] V. Calandrini, F. Arnesano, A. Galliani, T.H. Nguyen, E. Ippoliti, P. Carloni, G. Natile, Platination of Cu-transporter involved in anticancer drug resistance, Dalton Trans. 43 (2014) 12085–12094.
[15] E. Volckova, L.P. Dudones, R.N. Bose, HPLC determination of binding of cisplatin to DNA in the presence of biological thiols: implications of dominant platinum–thiol binding to its anticancer action, Pharm. Res. 19 (2002) 124–131.
[16] L. Galluzzi, I. Vitale, J. Michels, C. Brenner, G. Szabadkai, A. Harel-Bellan, M. Castedo, G. Kroemer, Systems biology of cisplatin resistance: past, present and future, Cell Death Dis. 5 (2014) e1257.
[17] M. Groessl, O. Zava, P.J. Dyson, Cellular uptake and subcellular distribution of ruthenium-based metallodrugs under clinical investigation versus cisplatin, Metallomics 3 (2011) 591–599.
[18] S. Sato, H. Fujiwara, T. Oishi, M. Shimada, S. Machida, Y. Takei, H. Itamochi, M. Suzuki, J. Kigawa, Evaluation of a formula for individual dosage of nedaplatin based on renal function, Cancer Chemother. Pharmacol. 69 (2012) 599–603.
[19] H. Kostrhunova, J. Kasparkova, D. Gibson, V. Brabec, Studies on cellular accumulation of satraplatin and its major metabolite JM118 and their interactions with glutathione, Mol. Pharm. 7 (2010) 2093–2102.
[20] R.N. Bose, L. Maurmann, R.J. Mishur, L. Yasui, S. Gupta, W.S. Grayburnb, H. Hofstetter, T. Salley, Non-DNA-binding platinum anticancer agents: cytotoxic activities of platinum–phosphato complexes towards human ovarian cancer cells, PNAS 105 (2008) 18314–18319.
[21] S. Moghaddas, P. Majmudar, R. Marin, H. Dezvareh, C. Qi, E. Soans, R.N. Bose, Phosphaplatins, next generation platinum antitumor agents: a paradigm shift in designing and defining molecular targets, Inorg. Chim. Acta 393 (2012) 173–181.
[22] D. Garcia Sar, M. Montes-Bayón, E. Blanco González, L.M. Sierra, L. Aguado, M.A. Comendador, S. Hann, G. Koellensperger, A. Sanz-Medel, Quantitative profiling of in-vivo generated cisplatin–DNA adducts using different isotope dilution strategies, Anal. Chem. 81 (2012) 9553–9560.
[23] S. Mowaka, M. Ziehe, D. Mohamed, U. Hochkirch, J. Thomale, M.W. Linscheid, Structures of oxaliplatin–oligonucleotide adducts from DNA, J. Mass Spectrom. 47 (2012) 1282–1293.
[24] M. Ziehe, D. Esteban-Fernández, U. Hochkirch, J. Thomale, M.W. Linscheid, On the complexity and dynamics of in vivo cisplatin-DNA adduct formation using HPLC/ICP-MS, Metallomics 4 (2012) 1098–1104.
[25] N. Sheppard, H.A. Willis, J.C. Rigg, Names, symbols, definitions and units of quantities in optical spectroscopy (Recommendations 1984), Pure Appl. Chem. 57 (1985) 105–120.
[26] A.E. Egger, C. Rappel, M.A. Jakupec, C.G. Hartinger, P. Heffeter, B.K. Keppler, Development of an experimental protocol for uptake studies of metal compounds in adherent tumor cells, J. Anal. At. Spectrom. 24 (2009) 51–61.
[27] W. Brüchert, R. Krüger, A. Tholey, M. Montes-Bayón, J. Bettmer, A novel approach for analysis of oligonucleotide–cisplatin interactions by continuous elution gel electrophoresis coupled to isotope dilution ICP-MS and MALDI-MS, Electrophoresis 29 (2008) 1451–1459.
[28] B. Stordal, N. Pavlakis, R. Davey, Oxaliplatin for the treatment of cisplatin-resistant cancer: a systematic review, Cancer Treat. Rev. 33 (2007) 347–357.